

# INTEGRATED DESIGN OF A VISION-GUIDED QUADROTOR UAV: A MECHATRONICS APPROACH

Abolfazl Mohebbi, Sofiane Achiche, Luc Baron

*Department of Mechanical Engineering, Ecole Polytechnique de Montreal, Montreal, Quebec, Canada*

*E-mails: abolfazl.mohebbi@polymtl.ca; sofiane.achiche@polymtl.ca; Luc.Baron@polymtl.ca*

---

## ABSTRACT

Designing Mechatronic systems is known to be both a very complex and tedious process due to the high number of system components, their multi-physical aspects, the couplings between the different domains involved in the product and the interacting design objectives. Due to this inherent complexity and the dynamic coupling between subsystems of mechatronic systems, a systematic and multi-objective design approach is crucial to replace the traditionally used sequential design methods that tend to deal with the different domains and their corresponding design objectives separately which usually leads to functional but not necessarily optimal designs solutions. In this paper, and based on an integrated and concurrent approach called "Design-for-Control" (DFC), a quadrotor UAV equipped with a stereo visual servoing system has been subjected to study for an optimal integrated design as an example for complex mechatronic system. After presenting the dynamics and control model of the quadrotor and its visual servoing system, the design process has been performed in four iterations and as expected, the control performance of the system has been significantly improved after finishing the final design iteration.

**Keywords:** Mechatronics; Integrated Design; Concurrent; Quadrotor; Visual Servoing.

---

## CONCEPTION INTÉGRÉE D'UN DRONE QUADRI-ROTOR ASSERVI PAR LA VISION ARTIFICIELLE : UNE APPROCHE MÉCATRONIQUE

### RÉSUMÉ

La conception de systèmes mécatroniques est à la fois un processus très complexe et fastidieux en raison du nombre élevé de composants système, leurs aspects multi-physiques, les couplages entre les différents domaines impliqués dans le produit et les objectifs de conception en interaction continue. En raison de cette complexité inhérente et le couplage dynamique entre les sous-systèmes mécatroniques, une approche de conception systématique et multi-objectif est essentielle pour remplacer les méthodes de design séquentielles traditionnellement utilisées qui ont tendance à traiter les différents domaines et leurs objectifs séparément, ce qui conduit généralement à des solutions fonctionnelles mais pas nécessairement optimales. Dans cet article, un drone de quadri-rotor équipé d'un système d'asservissement visuel stéréo a été soumis à l'étude pour une conception intégrée optimale basée sur une approche intégrée et simultanée appelé "Design-for-Control" (DFC). Le drone sert comme un exemple d'un système mécatronique complexe. Après avoir présenté le modèle dynamique et le contrôle de la quadri-rotor et son système d'asservissement visuel, le processus de conception a été réalisée en quatre itérations et les performances de commande du système ont été considérablement améliorées après avoir terminé la conception finale itération.

**Mots-clés :** Mécatronique, Conception intégrée, Drone, Asservissement visuel.

## NOMENCLATURE

Symbol	Description	Unit	Symbol	Description	Unit
$x, y, z$	Absolute position of CoG	m	$J_r$	Rotor inertia	kg.m <sup>2</sup>
$\phi, \theta, \psi$	Euler angles	rad	$J_m$	Motor inertia	kg.m <sup>2</sup>
$m$	Quadrotor overall mass	kg	$R$	Motor internal resistance	Ohm
$l$	Arm length	m	$r$	Gearbox reduction ratio	-
$\Omega_i$	speed of propeller-i	rad/s	$\gamma$	Gearbox efficiency	-
$\omega_m$	Motors angular speed	rad/s	$b_t$	Propeller Thrust factor	N.s <sup>2</sup>
$\tau_m$	Motors torque	N.m	$d$	Propeller Drag factor	N.m.s <sup>2</sup>
$\tau_d$	Motor load	N.m	$k_p$	Proportional control gain	-
$T_i$	Thrust of rotor - i	N	$k_d$	Derivative control gain	-
$I_{xx}$	Inertia moment on x axis	kg.m <sup>2</sup>	$k_i$	Integral control gain	-
$I_{yy}$	Inertia moment on y axis	kg.m <sup>2</sup>	$k_e$	Back-EMF constant	rad/V.s
$I_{zz}$	Inertia moment on z axis	kg.m <sup>2</sup>	$k_m$	Torque constant	N.m/Amp

## 1 INTRODUCTION

Due to the large number of couplings and interdependencies between elements and components, coming from different disciplines with different natures, design of Mechatronic systems is considered to be a highly complex task on various levels [1-3]. Therefore, in order to achieve a high precision and highly robust and efficient product, these couplings have to be considered in an early phase of the design process [4-6]. The main difficulty in the process of designing Mechatronic systems is that it requires a system perspective during all stages of design process in such a way that system interactions are considered, and a comprehensive system modeling is required. Design of a large number of modern mechatronic systems can be mapped into at least three aspects of structure or machine body, control system, and task. This design process has been traditionally performed in a sequential manner where the design of the structure is carried out first and then the control system design is performed. In such a sequential design process, once a mechatronic machine is developed, the mechanical structure can be hardly altered and all the mechanical parameters are time-invariant. A number of efforts have demonstrated that compared to systems designed by a traditional sequential approach, designing the structure and control in a concurrent process, considerably improves the system performance and efficiency [7-9]. Accordingly, the mechanical system design can contribute to the controller design and on the other hand, the behavior of control system can be studied to further improve the mechanical design to ideally improve the system performance. Integrated and concurrent design methodologies have been proposed over a number of works to optimally relate the mechanical and control components of mechatronic systems [10]. Due to their non-convex nature, many difficulties rise when solving optimization problems which simultaneously involve structural and control variables and parameters. Thus, despite the advances in optimal control design, optimal integrated Mechatronic system design is still an open research area. Toward the objective of optimal integrated design of Mechatronic systems, several investigations have been carried out in the past decade. In [11], authors first specified that the control system design could be simplified by incorporating the machine body design. In [12], a method to reduce the control effort and increase the dynamic performance of an actively controlled space structure is presented. With another application, a method of a mass-redistribution has been utilized in [13], to improve the motion tracking performance of manipulators. In [9] the control performance of a closed-chain machine has been improved by incorporating a PD control scheme along with a design approach of shaking force/shaking moment balancing.

A more general concept called *Design for Control* (DFC) was proposed in [14] where the design of the mechanical structure has been simplified as possible such that the dynamic modeling of the system will be less complex. Thus, a better control performance has been achieved. In this method the physical understanding of the overall system is fully explored with the aim of simplification of controller design as well as the execution of control algorithms with less hardware-in-the-loop restrictions. In [8, 15, 16],

specific design methods for machine body were proposed for the DFC approach based on considering invariant potential energy, invariant generalized inertia and partially invariant generalized inertia. In [10], a concurrent design approach is proposed to find the minimum positioning time of an underactuated manipulator where a synergetic combination between the structural parameters and a control law has been considered. In this paper, the integrated optimal design of a vision-guided UAV quadrotor is studied using the DFC approach. In terms of system dynamics, a quadrotor is an underactuated system with six degrees of freedom and four inputs which is inherently unstable and difficult to control. Thus, design and control of this nonlinear system is a problem for both practical and theoretical interests. Integrating the sensors, actuators and intelligence into a lightweight vertically flying system with a decent operation time is not trivial. Designing an autonomous quadrotor is basically a complex task since it requires dealing with numerous design parameters that are originated from various disciplines and subsystems and more importantly they are closely linked. Taking a decision about all these parameters requires a clear methodology. Moreover, In order to enable the system with autonomous capabilities, a visual feedback control will be used which increases the parameters of the system needed to be optimized. The rest of this paper is organized as follows; Section 2 of this paper recalls the dynamic model and formulations of a small quadrotor system. In Section 3, the control system design is presented. A formulation for image-based stereo visual servoing system is also presented in this section. In Section 4, the DFC-based integrated design strategy is introduced while in section 5 this method is utilized to optimize the integrated design of the quadrotor system. This section also includes validations with computer simulations. Finally, the concluding remarks are discussed in section 6.

## 2 SYSTEM MODELING AND FORMULATION

The design of quadrotor systems is a highly complex as various engineering domains and their affecting factors e.g. aerodynamics, mechanics, control and intelligence are involved in the design and optimization processes. The model of the quadrotor should consider all the important effects such as aerodynamic, inertial counter torques, friction, gyroscopic and gravitational effects on the final design solution. Euler-Lagrange formalism and DC motor equations are used to model the Quadrotor system. The dynamic model developed in this section is derived based on the following assumptions;

- The structure of the system is supposed to be rigid and symmetric.
- The thrust and drag affecting the system are proportional to the square of propellers speed [17].
- The origin of the body frame and the center of gravity (COG) are located at the same position.

Figure 1 illustrates the coordinate system for the quadrotor model in which  $W$  is the fixed world coordinate frame and  $B$  is the body fixed frame. The space orientation is also given by a rotation matrix  $R$  from frame  $B$  to  $W$ , where  $R \in SO3$ .

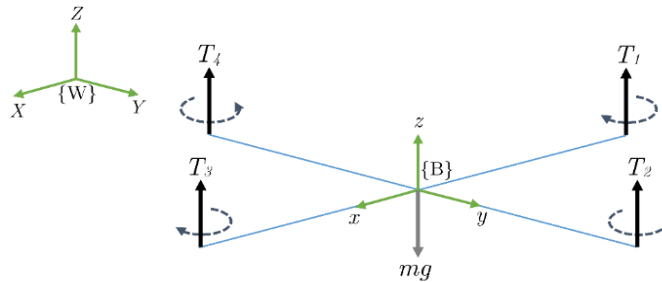


Figure 1. Quadrotor model coordinate system

For any point expressed in the fixed world coordinate frame, we can write (with, C:cos, S:sin);

$$\begin{cases} r_x = (C\psi C\theta) x + (C\psi S\theta S\phi - S\psi C\phi) y + (C\psi S\theta C\phi + S\psi S\phi) z \\ r_y = (S\psi C\theta) x + (S\psi S\theta S\phi + C\psi C\phi) y + (S\psi S\theta C\phi - C\psi S\phi) z \\ r_z = (-S\theta) x + (C\theta S\phi) y + (C\theta C\phi) z \end{cases} \quad (1)$$

The corresponding velocities are obtained by differentiation of Equation (1). From the obtained velocities and by assuming the inertia matrix to be diagonal, the kinetic and potential energy expressions can be written as follows:

$$T = \frac{1}{2} I_{xx} (\dot{\phi} - \dot{\psi} S \theta)^2 + \frac{1}{2} I_{yy} (\dot{\theta} C \phi + \dot{\psi} S \phi C \theta)^2 + \frac{1}{2} I_{zz} (\dot{\theta} S \phi - \dot{\psi} C \theta)^2 \quad (2)$$

$$V = \int x dm(x) (-g S \theta) + \int y dm(y) (g S \phi C \theta) + \int z dm(z) (g C \phi C \theta) \quad (3)$$

Using the Lagrangian function and the derived formula for the equations of motion we have:

$$L = T - V \quad , \quad Q_i = \frac{d}{dt} \left( \frac{\partial L}{\partial \dot{q}_i} \right) - \frac{\partial L}{\partial q_i} \quad (4)$$

where  $q_i$  are the generalized coordinates and  $Q_i$  are the generalized forces. Moreover, the non-conservative torques acting on the system result, firstly from the action of the thrust differences, Thus;

$$\tau_x = b_l l (\Omega_4^2 - \Omega_2^2), \quad \tau_y = b_l l (\Omega_3^2 - \Omega_1^2), \quad \tau_z = d (\Omega_2^2 + \Omega_4^2 - \Omega_1^2 - \Omega_3^2) \quad (5)$$

From the gyroscopic effects resulting from the propellers rotation we have:

$$\tau'_x = J_r w_y (\Omega_1 + \Omega_3 - \Omega_2 - \Omega_4), \quad \tau'_y = J_r w_x (\Omega_2 + \Omega_4 - \Omega_1 - \Omega_3) \quad (6)$$

Consequently, The quadrotor dynamic model describing the roll, pitch and yaw rotations contains then, three terms which are the gyroscopic effect resulting from the rigid body rotation, the gyroscopic effect resulting from the propeller rotation coupled with the body rotation and finally the actuators action. Applying small angle approximation we attain:

$$\begin{cases} \ddot{\phi} = \frac{J_r \dot{\theta} (\Omega_1 + \Omega_3 - \Omega_2 - \Omega_4)}{I_{xx}} + \frac{(I_{yy} - I_{zz})}{I_{xx}} \dot{\theta} \dot{\psi} + \frac{b_l l (\Omega_4^2 - \Omega_2^2)}{I_{xx}} \\ \ddot{\theta} = \frac{-J_r \dot{\phi} (\Omega_1 + \Omega_3 - \Omega_2 - \Omega_4)}{I_{yy}} + \frac{(I_{zz} - I_{xx})}{I_{yy}} \dot{\phi} \dot{\psi} + \frac{b_l l (\Omega_3^2 - \Omega_1^2)}{I_{yy}} \\ \ddot{\psi} = \frac{-d (\Omega_2^2 + \Omega_4^2 - \Omega_1^2 - \Omega_3^2)}{I_{zz}} + \frac{(I_{xx} - I_{yy})}{I_{zz}} \dot{\phi} \dot{\theta} \end{cases} \quad (7)$$

Using a Newton dynamics formulations we can also achieve:

$$\begin{pmatrix} \ddot{x} \\ \ddot{y} \\ \ddot{z} \end{pmatrix} = \begin{pmatrix} \frac{U_1}{m} (S \psi S \phi + C \psi S \theta C \phi) \\ \frac{U_1}{m} (-C \psi S \phi + S \psi S \theta C \phi) \\ -g + \frac{U_1}{m} (C \theta C \phi) \end{pmatrix} \quad (8)$$

The rotors are considered to be driven by DC-motors with the following well-known second order approximated equations which are linearized around an operation point  $\dot{w}_0$  :

$$\dot{w}_m = -A w_m + B u + C, \quad \text{where } A = \left( \frac{1}{\eta} + \frac{2dw_0}{\gamma r^3 J_r} \right), \quad B = \left( \frac{1}{k_m \eta} \right), \quad C = \left( \frac{dw_0^2}{\gamma r^3 J_r} \right), \quad \eta = \left( \frac{R J_r}{k_m^2} \right) \quad (9)$$

### 3 CONTROLLER DESIGN

The control system of the proposed quadrotor UAV here, consists of two components of motion control system and visual servoing (vision-based control) system. The cooperative configuration of these control systems is illustrated in a single control structure in Figure 2.

#### 3.1 Motion Control

In this study a PID controller is proposed for appropriate position control of the quadrotor. The dynamic model of the system, derived by any method, contains two gyroscopic effects. The influence of these effects in the present case and by considering a near-hover situation, is less important than the motor's model. Thus, using motor inputs  $\Omega_i$ , the rotational transfer functions can be described by:

$$\phi(s) = \frac{B^2 lb}{s^2 (s + A)^2 I_x} (\Omega_4^2(s) - \Omega_2^2(s)) \quad (10)$$

$$\theta(s) = \frac{B^2 l}{s^2 (s + A)^2 I_y} (\Omega_3^2(s) - \Omega_1^2(s)) \quad (11)$$

$$\psi(s) = \frac{B^2 d}{s^2 (s + A)^2 I_z} (\Omega_2^2(s) + \Omega_4^2(s) - \Omega_1^2(s) - \Omega_3^2(s)) \quad (12)$$

Where A and B are the coefficients of the linearized rotor dynamics from Equation 10. The transfer function of a PID controller is found by taking the Laplace transform of the last equation;

$$PID = G_{C,\phi}(s) = (k_p + \frac{k_i}{s} + k_d \cdot s) = \frac{k_d s^2 + k_p s + k_i}{s} \quad (13)$$

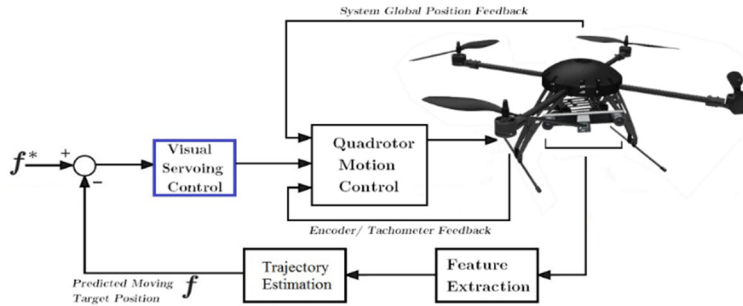


Figure 2. Quadrotor control structure schematic consisting of attitude motion control and visual servoing control

### 3.2 Visual Servoing Control

In general it can be stated that in an image-based visual servoing system, the goal of vision-based control scheme is to minimize the error defined as:

$$e(t) = s - s^* \quad (14)$$

where  $s$  and  $s^*$  are the vectors of current and desired image features. In the case of a proportional controller, the input to the robot controller  $u_c$  (camera frame velocities) is designed by letting  $\dot{e} = -\lambda e$ :

$$u_c = -\lambda J_e^+ e, \quad (15)$$

where  $J_e$  is the image interaction matrix which relates time variation of  $e$  and the camera velocity and  $J_e^+$  is the Moore-Penrose pseudo-inverse of interaction matrix. In the case of moving features we have:

$$u_c = J_e^+ \left( -\lambda e - \frac{\partial e}{\partial t} \right) \quad (16)$$

where the term  $(\partial e / \partial t)$  represents the time variation of  $e$  caused by the target motion which is considered to have a constant velocity. In our case we assume that the vision system is composed of a stereo vision system with two parallel cameras which are perpendicular to the baseline. The focal points of two cameras are apart at distance  $b/2$  with respect to origin of sensor frame  $C$  on the baseline which means the origin of the camera frame, is in the center of these points. Focal distance of both cameras is  $f$ . We assign  $L$  and  $R$  as the frames of the left and right images. Figure 3 illustrates the case where both cameras observe a 3D point  ${}^C P$ . Using the image interaction matrices for the left and right cameras and also a camera projection model, the stereo image interaction matrix,  $J_{st}$ , can be calculated as:

$$J_{st} = (J_l {}^l M_C, J_r {}^r M_C)^T \quad (17)$$

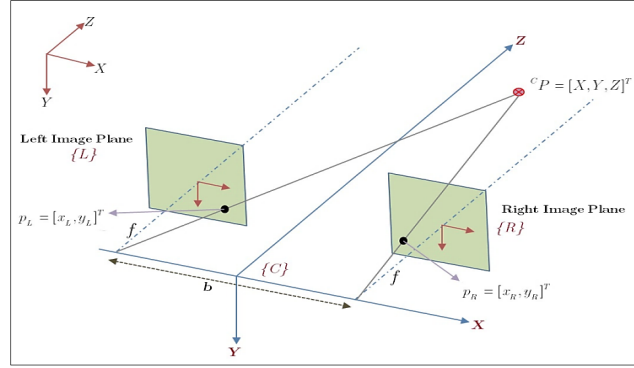


Figure 3. Model of the parallel stereo vision system observing a 3D point

The image interaction matrix for each camera is calculated as:

$$J_i = \begin{pmatrix} \frac{-1}{Z_i} & 0 & \frac{x_i}{Z_i} & x_i y_i & -(1 + x_i^2) & y_i \\ 0 & \frac{-1}{Z_i} & \frac{y_i}{Z_i} & 1 + x_i^2 & -x_i y_i & -x_i \end{pmatrix} \quad (18)$$

The stereo feature vector is defined as  $s = [x_l, y_l, x_r, y_r]^T$  where  $p_l = [x_l, y_l]^T$ ,  $p_r = [x_r, y_r]^T$  are the normalized image coordinates of the 3D point, observed by the left and right cameras respectively. A perspective camera model can be used to project observed point into left and right image planes. Thus, the following equations hold for 3D coordinates of the observed point:

$$(X, Y, Z) = \left( \frac{b}{2} \frac{x_l + x_r}{x_l - x_r}, Y = y_l \frac{b}{x_l - x_r}, Z = \frac{b}{x_l - x_r} \right) \quad (19)$$

#### 4 INTEGRATED DESIGN STRATEGY

An engineering design process can be parametrically defined as a mapping from a requirement space consisting of behaviors to a structural parameter space [18]. To gain insight into the design of a mechatronic system, Li *et al.* [14] suggested dividing the requirement space into two subspaces which represent: Real-time behaviors (RTBs) and Non-real-time behaviors (Non-RTBs). Following this division of the requirements, system parameters in structural space can also be divided into two subspaces as follows: Real-time controllable parameters (RTPs) and Nonreal-time uncontrollable parameters (Non-RTPs). Here, “real-time” means parameters, specifications, constraints and behaviors that may change with time after the machine is built. Controller gains, accuracy and speed are some examples of RTPs and RTBs. On the other hand, Nonreal-time parameters, constraints and specifications are the ones that should not be changed after the machine is built, because it would be costly to change them. Structural material, dimensions, weight, and workspace can be considered as Non-RTPs and Non-RTBs. Traditional methodologies for mechatronic systems design consisted of sequences of the real-time and non-real-time requirements rather than a concurrent design process. At the beginning of such a traditional design scenario, Non-RTPs are designed based on the Non-RTB specifications. This process itself includes designing the mechanical structure and then adding electrical components. The mechanical structure (e.g., configurations, dimensions, layout of actuators and sensors, etc.) is first determined based on the requirements in the Non-RTB space (e.g., workspaces, maximum payloads, etc.). Subsequently, RTPs (e.g., controller algorithm and parameters, signal conditioning) are determined based on RTB specifications (e.g., desired trajectory, speed, stability, etc.) to control the already established structure. Due to recent advancements in control and computer engineering one may conclude that the design of the imperfections and inadequacies in

structure and hardware of a Mechatronic system can be compensated by some state-of-the-art control schemes. This thinking can be easily criticized because a perfect control response may be hardly achieved due to hardware limitations and dynamic interactions, regardless of the effort devoted to the design of the controller system. In a concurrent model for mechatronic systems design, both RTBs and Non-RTBs should be considered simultaneously for realization of RTPs and Non-RTPs. In a general Mechatronic system, the system performance which is the real-time and nonreal-time system behaviors (RTBs and Non-RTBs) explicitly relies on the design of its control algorithm and parameters (RTPs) and the design of the mechanical structure (Non-RTPs). More specifically, the design specifications for controller and limitations should be considered in the design of the mechanical structure and in the considering the alternatives for the electrical hardware. In addition, unlike in a traditional design, controllability and programmability of RTPs should be considered as an opportunity to further improve the design after the machine is built. Let  $X_R$  and  $X_N$  be RTP and Non-RTP design vectors. We also assume there exist  $n$  RTPs and  $m$  NonRTPs, that is  $X_R \in R^n$ , and  $X_N \in R^m$ , where the total number of design parameters is  $q=m+n$ . respectively, the determination of design parameters is subject to a set of constraints produced by the behavior requirements. Thus, let  $Y_R$  and  $Y_N$  denote  $u$ -RTB and  $v$ -NonRTB requirements which sums to  $p=u+v$  as the total number of variables in the requirement space. Thus,  $Y_R \in R^u$ , and  $Y_N \in R^v$ . Assuming  $Y = [Y_R, Y_N]$ , the performance error can be defined as  $E = Y - Y_d$  where  $Y_d$  is the vector of desired behaviors. Accordingly, Let  $S_{\min}$  and  $S_{\max}$  denote the design requirements associated with a particular design problem, where “min” and “max” indicate the performance indices of the requirements to be minimized and maximized, respectively. Finally, let  $P$  denote the system actuation power. A Mechatronic system design problem can be described using the following mathematical models for objectives and constraints [14]:

$$E = \min \sum_{i=1}^p \alpha_i |E_R|_i + \xi_i |E_N|_i \quad (20)$$

$$P = \min \sum_{i=1}^{dof} \beta_i p_i \quad (21)$$

$$S_{\min} = \min \sum_{i=1}^{q1} \lambda_i |S_{\min}|_i \quad (22)$$

$$S_{\max} = \max \sum_{i=1}^{q2} \rho_i |S_{\max}|_i \quad (23)$$

$$I = E + P + S_{\min} - S_{\max} \quad (24)$$

where  $\alpha_i, \xi_i, \beta_i, \lambda_i, \rho_i$  are weighting factors determined by the designer,  $p_i$  is the power generated by each actuator in the system and  $q1$  and  $q2$  are the number of the design parameters associated with the minimized and maximized requirements. To optimize the overall design performance, a performance index ( $I$ ) is introduced to integrate are introduced individual objectives in one equation. The equality and inequality constraints can be respectively expressed by:

$$Y_R^E = f_R^E(X_R, X_N), \quad Y_N^E = f_N^E(X_N) \quad (25)$$

$$Y_{R,low} < f_R^I(X_R, X_N) < Y_{R,up}; \quad Y_{N,low} < f_N^I(X_N) < Y_{N,up} \quad (26)$$

Where the superscript “I” indicates the inequality constraints and the superscript “E” indicates the equality constraints. From the above design constraints it can be observed that, for a Mechatronic system, the system dynamic performance (RTBs or  $Y_R$ ) depends on both the control parameters (RTPs or  $X_R$ ) and the mechanical structure behaviors (NonRTPs or  $Y_N$ ). As stated before, the essence of DFC method is to design

the mechanical structure ( $X_N$ ) in an effort to achieve a simple dynamic model for the ease of designing the control system ( $X_R$ ), to ideally achieve an optimal system dynamic performance ( $Y_R$ ). In a simulation-based iterative integrated design strategy,  $X_N$  is first set for a mechanical structure based on the desired behaviors and requirements (associated with  $Y_N$  directly yet  $Y_R$  indirectly). Then having  $X_R$  determined, the dynamic performance  $Y_2$  is obtained (based on  $Y_R$  explicitly and  $Y_N$  implicitly). In the third step,  $Y_N$  will be configured by comparing the desired behaviors with the measured ones. If the result is not satisfactory, then  $X_R$  is modified to improve the control performance. Finally in the fourth step, if the control performance  $Y_3$  does not satisfy the requirements,  $X_R$  is varied again to attain an improved performance. All of the aforementioned four design steps can be summarized as:

$$Y_1 = f_1(X_N) \rightarrow Y_2 = f_2(Y_2, X_R) \rightarrow Y_3 = f_3(Y_2, X_N) \rightarrow Y_4 = f_4(Y_3, X_R). \quad (27)$$

For an algorithmic implementation, the iterations can be formulated as:

$$Y_{2i-1} = f_{2i-1}(Y_{2i-2}, X_N) ; Y_{2i} = f_{2i}(Y_{2i-1}, X_R) \quad \text{for } (i = 1, 2, \dots, k) \quad (28)$$

The design procedure iterates until a final design on  $X_R$  is found that enables the system to achieve a satisfactory performance. When an analytical system dynamic model is obtainable, the iterative design process described before can be carried out via simulation process.  $X_N$  can be further changed towards various directions along the searching path. It is quite possible to find a solution to the optimal design problem with the fewest constraints. Having the dynamics model,  $X_N$  can be varied until a simpler dynamic model can be achieved which results in facilitating the procedure of control system design.

## 5 DFC-BASED DESIGN OPTIMIZATION

Using the Design-for-Control (DFC) approach, an integrated design of a vision-guided quadrotor UAV is studied in this paper. The first column of Table 1 classifies all the RTPs and Non-RTPs, as the design parameters in the process of designing a vision-guided quadrotor drone with a PID attitude control system. After identifying all the parameters and behaviors, the integrated design iterations are as follows:

### 5.1 Iteration 1: Design $X_N$ Based on Non-RTBs, $Y_N$ :

The first step is to determine  $X_N$ , the mechanical structure parameters, so that the specified Non-RTBs,  $Y_N$ , are satisfied. As the first requirement, the quadrotor is subjected to the following constraints;

$$0.2 \leq l \leq 0.4 \text{ (m)}, \quad m_t \geq 0.4 \text{ (kg)}, \quad 0.006 \leq I_{xx}, I_{yy} \leq 0.01 \text{ (kg.m}^2\text{)} \quad (29)$$

Where the inertia moments can be calculated from a simple physical model of the quadrotor where it consists of two rods as the arms, one disk at center and four concentrated mass at the end of each arm. One of the major physical limitations of a quadrotor is the propeller's rotational speed which is constrained by the motor saturation speed. This saturation speed of the propellers should be approximately 41% higher than the hovering speed [19]. The propeller's rotational speed in hovering condition is obtained by:

$$\Omega_H = (mg / 4b_t)^{1/2} \quad (30)$$

Thus, having the condition of  $\Omega_i \leq 350 \text{ (rad / s)}$  and also the trust factor  $b_t=3.15E-5$  we can achieve an allowable total mass and payload capacity:

$$m \leq \frac{4b_t \Omega_{i,\max}^2}{g(1.41)^2} = 0.791 \text{ (kg)} \quad (31)$$

Having the aforementioned Non-RTB constraints the first set of Non-RTPs can be chosen as the starting point of the optimization problem. The design result of  $X_N$  is given in the first column of Table 1.



## 5.2 Iteration 2: Design $X_R$ Based on RTBs, $Y_R$ :

Once the initial design of the mechanical structure is completed, the motion controller and visual servoing system must be designed carefully such that the required dynamic and visual performances are satisfied. Thus, the design objective is to minimize the performance index over the entire range of motion:

$$I_R = E_R^Q + E_R^C + P \quad (32)$$

$$E_R^Q = \min \left( \alpha_1 \int_0^{t_f} ((X(t) - X_d)^2 + (Y(t) - Y_d)^2 + (Z(t) - Z_d)^2) dt + \alpha_2 \int_0^{t_f} ((\dot{X}(t) - \dot{X}_d)^2 + (\dot{Y}(t) - \dot{Y}_d)^2 + (\dot{Z}(t) - \dot{Z}_d)^2) dt \right) \quad (33)$$

$$E_R^C = \min \left( \alpha_3 \int_0^{t_f} (s(t) - s^*)^2 dt \right) \quad (34)$$

$$P = \min \left( \beta \int_0^{t_f} |T_i(t)| dt \right) \quad (35)$$

Where  $E_R^Q$  is the minimum performance error for position and velocity tracking and  $E_R^C$  is the minimum performance error for the visual servoing system.  $P$  signifies the driving torque generated by the motion control, and  $\alpha_i, \beta$  are the weighting factors to be determined. Accordingly, the following RTB constraints (control inputs) are imposed on the controller design:

$$0 \leq \sum T_i \leq 2mg \quad (36)$$

$$|\phi| \leq 0.6 \text{ rad}, \quad |\theta| \leq 0.6 \text{ rad}, \quad 0 \leq \psi \leq 0.01 \text{ rad} \quad (37)$$

For translational speed and descend rate we also have:

$$|\dot{x}| \leq 10 \text{ m.s}^{-1}, \quad |\dot{y}| \leq 10 \text{ m.s}^{-1}, \quad |\dot{z}| \leq 5 \text{ m.s}^{-1} \quad (38)$$

The target object which is being tracked by the vision system is moving along a circle path on x-y plane with the radius of 4 meters and the quadrotor is required to follow the target with the height of 2 meters with respect to target. The target object is travelling with the speed of 10 m/s along the circular path and the quadrotor is not allowed to have a translational speed more than the object. In order to simplify the problem no minimum time-trajectory is given. The control design problem is solved using MATLAB optimization toolbox. To ensure each performance characteristic (i.e.  $E_R^Q, E_R^C$  and  $P$ ) contributes properly to the performance index in an equivalent magnitude, the weighting factors are selected to be  $\alpha_1 = 1.0, \alpha_2 = 0.1, \alpha_3 = 0.5, \beta = 0.005$ . The design result of  $X_R$  is given in the second column of Table 1. The simulation model built in MATLAB to reflect the design process results is shown in Figure 4 (a). Using the control gains as a result from the aforementioned optimization solution, the tracking performances for both motion and vision-based control are comparatively displayed in Figures 4 and 5 and as it can be observed some undesired performance appears in the position tracking and the visual features error are also not quite satisfactory.

## 5.3 Iteration 3: Redesign $X_N$ to Improve Non-RTBs, $Y_N$ :

In the third iteration the NonRTPs,  $X_N$ , will be modified with the aim of simplifying the system dynamic model so that the controller design on  $X_R$  can be facilitated. In this redesign, the following stability constraints are used for the modification of  $X_N$  [20];

$$\frac{g}{I_{xx}} \frac{\partial \phi}{\partial \dot{y}} > 0, \quad \frac{g}{I_{yy}} \frac{\partial \theta}{\partial \dot{x}} > 0. \quad (39)$$

The dynamic model can be finally simplified as:

$$I_{xx} \ddot{\phi} = \dot{\theta} \dot{\psi} (I_{yy} - I_{zz}), \quad I_{yy} \ddot{\theta} = \dot{\phi} \dot{\psi} (I_{zz} - I_{xx}), \quad I_{zz} \ddot{\psi} = \dot{\phi} \dot{\theta} (I_{xx} - I_{yy}). \quad (40)$$

The redesigned values of  $X_N$  is now given in the third column of Table 1.

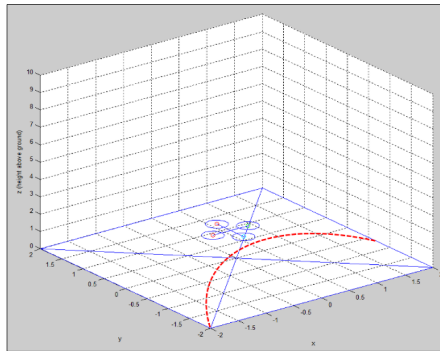
#### 5.4 Iteration 4: Redesign $X_R$ based on the modified Non-RTBs, $Y_N$ :

After the redesigning the Non-RTPs,  $X_N$ , the visual servoing and motion control algorithm are again applied for the path and trajectory tracking of the target object. In this iteration, the design objective, constraints, and variables are the same as those in Iteration 2. The design result of control gains,  $X_R$ , is given in the fourth column of Table I, which is the same as the control gains used in Iteration 3. The new tracking performances are also displayed in Figures 4 and 5. Compared with the results of Iteration 2, it can be observed that the position tracking performance has been enhanced and the performance with regards to visual features errors has also shown better convergence characteristics.

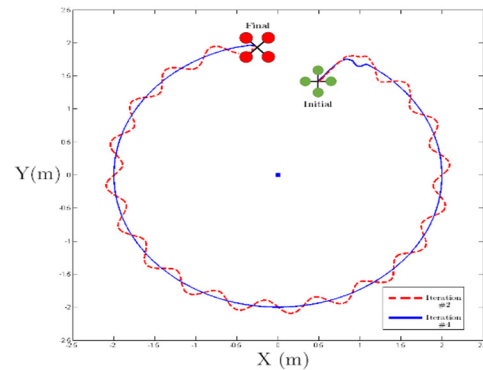
Table 1. DFC-based design of a vision-guided quadrotor system: results for all iterations

Non-RTPs	Descriptions	Iteration 1	Iteration 2	Iteration 3	Iteration 4
$l$	Arm length (m)	0.25	/	0.28	/
$m$	Total mass (kg)	0.65	/	0.72	/
$I_{xx}$	Inertia moments on x (kg.m <sup>2</sup> )	0.009	/	0.0076	/
$I_{yy}$	Inertia moments on y (kg.m <sup>2</sup> )	0.008	/	0.0076	/
$I_{zz}$	Inertia moments on z (kg.m <sup>2</sup> )	0.017	/	0.0152	/
$b$	Distance between cameras (m)	0.15	/	0.1	/
RTPs					
$k_p$	Proportional control gain	/	1.5	/	1.3
$k_d$	Integral control gain	/	1.0	/	0.8
$k_i$	Derivative control gain	/	0.6	/	0.4
$\lambda$	Proportional gain in visual servoing	/	0.5	/	0.35

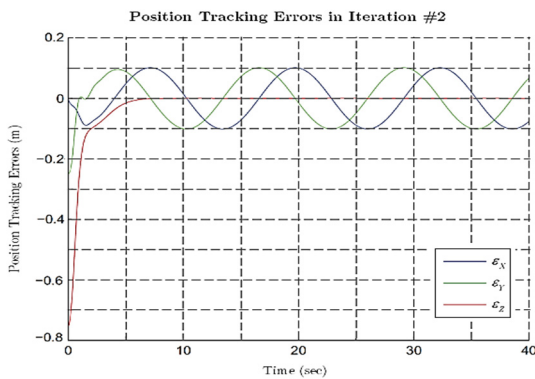
It can be observed that after a limited number of iterations, the obtained design variables are quite satisfactory and elevate the performance of the proposed system. However, this will hold only for systems with small number of components and consequently design variables and parameters. Using the DFC method for more complicated mechanisms with complex control systems is not easy to implement and will require the designer to set a large number of constants and this will definitely cause the whole design process to need more iterations, not taking into accounts the new constraints which will be introduced to the optimization process. This will call for some additional efforts to establish guidelines for choosing those constants and more importantly, a faster and more “integrated” approach, as future efforts.



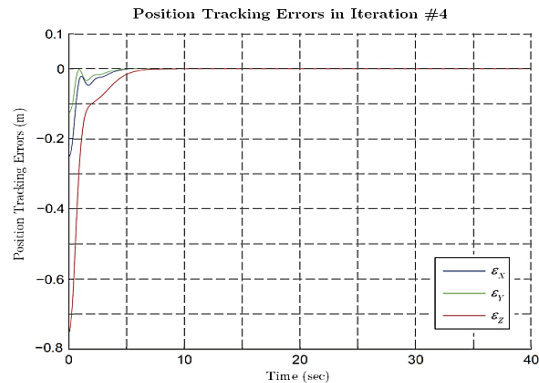
(a)



(b)

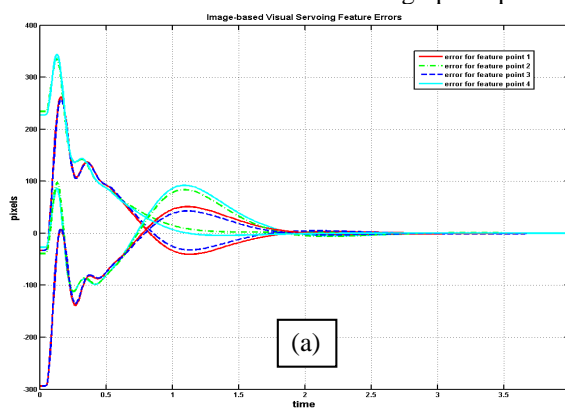


(c)

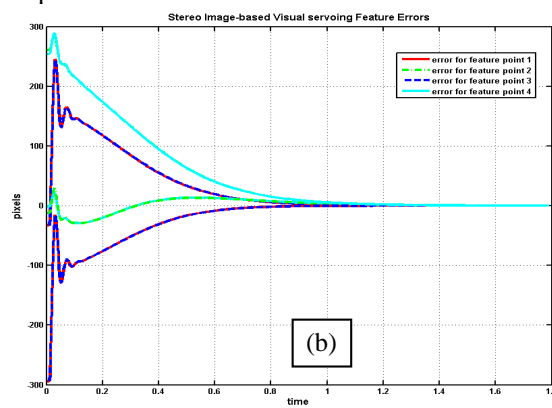


(d)

Figure 4. Position tracking performances based on results from (a) iteration 2 and (b) iteration 4, and a comparative graph of paths for a complete motion.



(a)



(b)

Figure 5. Visual feature errors from (a) iteration 2 and (b) iteration 4.

## 6 CONCLUSIONS

In this paper, the problem of integrated and concurrent design of a vision-guided quadrotor UAV has been studied using the Design-for-Control methodology. This method suggests considering the design of a mechatronic system as a mapping from a requirement space to a structure space. The mechatronic design concept is therefore interpreted as an integrated design framework that considers both real-time and nonreal-time requirements simultaneously and configures both real-time and nonreal-time parameters (design variables) concurrently. Having discussed the design approach, the concurrent design of both mechanical and control structures of a vision-guided quadrotor system has been accomplished in an iterative manner and after finalizing the last iterations, desired performances with regards to both control systems, i.e. motion control and visual servoing, have been achieved. However, for systems with larger number of components and more complex control systems, additional efforts to establish guidelines for choosing the design optimization constants, hence a more “integrated” approach, is ideally required.

## REFERENCES

- [1] J. M. r. Torry-Smith, S. Achiche, N. H. Mortensen, A. Qamar, J. Wikander, and C. During, "Mechatronic Design-Still a Considerable Challenge," in *ASME 2011 International Design Engineering Technical Conferences and Computers and Information in Engineering Conference*, 2011, pp. 33-44.
- [2] J. M. Torry-Smith, A. Qamar, S. Achiche, J. Wikander, N. H. Mortensen, and C. During, "Challenges in designing mechatronic systems," *Journal of Mechanical Design*, vol. 135, p. 011005, 2013.

- [3] A. Mohebbi, S. Achiche, L. Baron, and L. Birglen, "Trends in concurrent, multi-criteria and optimal design of mechatronic systems: A review," in *Innovative Design and Manufacturing (ICIDM), Proceedings of the 2014 International Conference on*, 2014, pp. 88-93.
- [4] A. Mohebbi, S. Achiche, and L. Baron, "Mechatronic Multicriteria Profile (MMP) for Conceptual Design of a Robotic Visual Servoing System," in *ASME 2014 12th Biennial Conference on Engineering Systems Design and Analysis*, 2014, pp. V003T15A015-V003T15A015.
- [5] A. Mohebbi, S. Achiche, L. Baron, and L. Birglen, "Neural network-based decision support for conceptual design of a mechatronic system using mechatronic multi-criteria profile (MMP)," in *Innovative Design and Manufacturing (ICIDM), Proceedings of the 2014 International Conference on*, 2014, pp. 105-110.
- [6] A. Mohebbi, S. Achiche, L. Baron, and L. Birglen, "Fuzzy Decision Making for Conceptual Design of a Visual Servoing System Using Mechatronic Multi-Criteria Profile (MMP)," in *ASME 2014 International Mechanical Engineering Congress and Exposition*, 2014, pp. V011T14A055-V011T14A055.
- [7] H.-S. Yan and G.-J. Yan, "Integrated control and mechanism design for the variable input-speed servo four-bar linkages," *Mechatronics*, vol. 19, pp. 274-285, 2009.
- [8] L. Cheng, Y. Lin, Z.-G. Hou, M. Tan, J. Huang, and W. Zhang, "Integrated design of machine body and control algorithm for improving the robustness of a closed-chain five-bar machine," *Mechatronics, IEEE/ASME Transactions on*, vol. 17, pp. 587-591, 2012.
- [9] W. Zhang, Q. Li, and L. Guo, "Integrated design of mechanical structure and control algorithm for a programmable four-bar linkage," *Mechatronics, IEEE/ASME Transactions on*, vol. 4, pp. 354-362, 1999.
- [10] C. A. Cruz-Villar, J. Alvarez-Gallegos, and M. G. Villarreal-Cervantes, "Concurrent redesign of an underactuated robot manipulator," *Mechatronics*, vol. 19, pp. 178-183, 2009.
- [11] K. Youcef-Toumi and A. T. Y. Kuo, "High-speed trajectory control of a direct-drive manipulator," *Robotics and Automation, IEEE Transactions on*, vol. 9, pp. 102-108, 1993.
- [12] W. K. Belvin and K. Park, "Structural tailoring and feedback control synthesis-An interdisciplinary approach," *Journal of Guidance, Control, and Dynamics*, vol. 13, pp. 424-429, 1990.
- [13] H. Diken, "Trajectory control of mass balanced manipulators," *Mechanism and Machine Theory*, vol. 32, pp. 313-322, 4// 1997.
- [14] Q. Li, W. Zhang, and L. Chen, "Design for control-a concurrent engineering approach for mechatronic systems design," *Mechatronics, IEEE/ASME Transactions on*, vol. 6, pp. 161-169, 2001.
- [15] Q. Li and F. Wu, "Control performance improvement of a parallel robot via the design for control approach," *Mechatronics*, vol. 14, pp. 947-964, 2004.
- [16] F. Wu, W. Zhang, Q. Li, and P. Ouyang, "Integrated design and PD control of high-speed closed-loop mechanisms," *Journal of dynamic systems, measurement, and control*, vol. 124, pp. 522-528, 2002.
- [17] S. Bouabdallah, A. Noth, and R. Siegwart, "PID vs LQ control techniques applied to an indoor micro quadrotor," in *Intelligent Robots and Systems, 2004. (IROS 2004). Proceedings. 2004 IEEE/RSJ International Conference on*, 2004, pp. 2451-2456 vol.3.
- [18] N. P. Suh, *The Principles of Design*: Oxford University Press on Demand, 1990.
- [19] M. Cutler, N. K. Ure, B. Michini, and J. P. How, "Comparison of fixed and variable pitch actuators for agile quadrotors," in *AIAA Guidance, Navigation, and Control Conference (GNC), Portland, OR*, 2011.
- [20] P. E. I. Pounds, "Design, construction and control of a large quadrotor micro air vehicle," Australian National University, 2007.